Comparison of optoelectrical characteristics between Schottky and Ohmic contacts to -Ga₂O₃ thin film

Comparison of optoelectrical characteristics between Schottky and Ohmic contacts to β-Ga_2O_3 thin film

Zeng Liu[1], Yusong Zhi[1], Shan Li[1], Yuanyuan Liu[2,5], Xiao Tang[3], Zuyong Yan[1], Peigang Li[1], Xiaohang Li[3], Daoyou Guo[4], Zhenping Wu[1] and Weihua Tang[1]

[1] Laboratory of Information Functional Materials and Devices, School of Science & State Key Laboratory of Information Photonics and Optical Communications, Beijing University of Posts and Telecommunications, Beijing 100876, People's Republic of China

[2] Center of Materials Science and Optoelectronics Engineering, University of Chinese Academy of Sciences, Beijing 100049, People's Republic of China

[3] Advanced Semiconductor Laboratory, King Abdullah University of Science and Technology (KAUST), Thuwal 23955-6900, Saudi Arabia

[4] Center for Optoelectronics Materials and Devices, Department of Physics, Zhejiang Sci-Tech University, Hangzhou 310018, People's Republic of China

[5] The Engineering Research Center for Semiconductor Integrated Technology, Institute of Semiconductors, Chinese Academy of Sciences, Beijing 100083, People's Republic of China

E-mail: zengliu@bupt.edu.cn, pgli@bupt.edu.cn and whtang@bupt.edu.cn

Abstract

Schottky and Ohmic contacts are key matters affecting carrier transport in oxide semiconductor based electrical and optical devices. For Ga_2O_3, the comparison of optoelectrical behaviors and the fundamental physical mechanism between these two contacts are not well known yet. In this work, β-Ga_2O_3 thin films were grown via metal-organic chemical vapor deposition then deposited with symmetrical Ni/Au (Schottky) or Ti/Au (Ohmic) contacts. Optoelectrical measurements show that the Ohmic contacted device exhibits superior responsivities thanks to their higher photocurrents. While for the Schottky contacted device, firstly, it has faster response speed, secondly it exhibits larger photo-to-dark current ratios owing to their low dark current. Specifically, the voltage- and light intensity-dependent responsivity and detectivities of the Schottky and Ohmic contacted devices were measured and discussed under the consideration of different voltages and UV light intensities.

Keywords: β-Ga_2O_3, Schottky and Ohmic contacts, optoelectrical characteristics, metal-organic chemical vapor deposition (MOCVD)

1. Introduction

Due to the promising applications in information communications, chemical/biological analysis, flame detection, and environmental protection, ultraviolet (UV) photodetectors have drawn extensive research interests in the past years. Among them, the UV solar-blind detectors operating

in a wavelength range from 200 nm to 280 nm are the solid choice for ozone sensing with low false alarming rate [1-3]. The performances of photodetectors, to a large degree, depend on the nature and modified properties of the selected materials [4]. Specifically, as one of the typical wide bandgap semiconductors, β-Ga_2O_3 not only has a ultra-wide bandgap of 4.5-4.9 eV (responding in the UV solid-blind regime), but also high thermal and chemical stability, high critical breakdown field of 6-8 MV/cm (allowing high voltage and strong radiation operations) [5, 6], therefore allowing them extensively employed to fabricate UV solar-blind photodetectors [7] in the forms of thin films [8-12], bulk single crystals [13-16] nanostructures [17-20] and heterogeneous structures [20-26].

Metal-Semiconductor-Metal (MSM) structure is a typically and widely used electrode pattern in photodetectors [27], in which either Ohmic or Schottky metal-semiconductor (M-S) contacts are employed in line with the requirements of the applications. The Ohmic contacted detectors (regarding as radiation-sensitive resistors), referenced as photoconductive, are presented by the change of resistance of the materials due to the external light stimulation, showing the intrinsic feature of materials [1, 8, 28, 29]. While the Schottky contacted detectors could show some modified performances owing to the efficient control of carrier transport via tuning the M-S interface barrier and the thickness of the depletion layer at the M-S interface [29-31]. For instance, Guo *et al* grew β-Ga_2O_3 thin film by laser molecular beam epitaxy and displayed a good Ohmic electrical behavior with dark current of 45 nA and rise time of 1.91 s, while the Schottky M-S behavior was illustrated after annealing, and the dark current and rise time were changed to be 0.3 nA and 0.62 s, respectively [8]. Other than the semiconductor and/or device processing, the contacting types depend on the choice of contacted metals [32], i.e., the difference between the work function of metal and the electron affinity of Ga_2O_3. An *et al* achieved good Ohmic contact in their photodetector, this device shown decent photoresponsivity and wavelength selectivity, while a long response time of 19 s [33]. As opposed to this, Chen *et al* demonstrated a fast responding Au/β-Ga_2O_3 nanowires array photodetector with faster decay time of 64 μs [34]. Such a UV detector may be contributed to the development of a depletion layer at the Au/β-Ga_2O_3 interface, which could restrain the separation of electron-hole pairs and conduce to the practicability more easily. In all, the M-S contact is a vital matter to determine the carrier transport and then affect the detector performances [35-39], due to

the differences between work function of metals and electron affinity of Ga_2O_3. However, to the best of our current knowledge, a systematic comparison of Schottky and Ohmic contacts to Ga_2O_3 and the influences on photodetector performances are less reported.

In this work, β-Ga_2O_3 thin films were grown via metal-organic chemical vapor deposition (MOCVD) then deposited with Ni/Au (Schottky) or Ti/Au (Ohmic) contacts. The optoelectrical behaviors, photogenerated currents, time-dependent photoresponse, photoreponsivities, detectivities, response time were systematically measured on the as-prepared devices. These aforementioned performances of the Ni/Au (Schottky) and Ti/Au (Ohmic) contacted devices were systematically compared and discussed. In addition, the inherent physical mechanism of this practical phenomenon was elucidated for its further optoelectronic applications.

2. Experimental

The deposition of β-Ga_2O_3 thin film on c-plane sapphire substrate was performed via a customized MOCVD thin film growth system with a close-coupled showerhead reactor. Triethylgallium (TEGa) and high-purity (5N) oxygen gas were used as gallium and oxygen sources, respectively. TEGa was stored in a stainless steel bubbler, which was kept at temperature of 35 ℃ and pressure of 760 Torr. Oxygen gas was delivered into the growth chamber, and a gas ratio of 6000 SCCM was set. On the basis of the set oxygen flow, the [O/Ga] molar ratio was regulated to be ~1657. Specifically, according to the Antoine's equation $\log(P_{MO}) = a - b/T$ [41, 42], where P_{MO} is the vapor pressure of TMGa, a and b are the Antoine constants, and T is the thermodynamic temperature of TMGa. $n_{mo} = \frac{F \times P_{MO}}{V_m \times (P_{bub} - P_{MO})}$, where n_{mo} is the molar flow rate of TMGa, F is the flow rate of carrier gas, V_m = 22414 cm^3/mol (ideal gas molar volume), P_{bub} is the pressure inside the bubbler. $n_{O2} = \frac{F_O}{V_m}$, where n_{O2} is the molar flow rate of O_2, F_O is the flow rate of O_2. Therefore, the [O/Ga] molar ratios in the experiment could be expressed as: [O/Ga] = $\frac{n_{O2}}{n_{mo}} = \frac{5.35 \times 10^{-1}}{3.23 \times 10^{-4}} \sim 1657$. The growth process was maintained for 15 min under a fixed growth chamber condition with temperature of 735 ℃ and pressure of 25 Torr.

The symmetrical Ni/Au and/or Ti/Au metal electrodes were patterned on the surface of β-Ga_2O_3 thin film by means of electron beam evaporation, conventional photolithography and lift-off techniques. The same photomask was employed to pattern the Ni/Au (120 nm/180 nm) and Ti/Au

(120 nm/180 nm) metal electrodes. The quadrate electrodes are 400 μm wide and 400 μm long, and 200 μm spacing gap. Calculated from the scale of electrode patterns, the efficient irradiant area could be about 8×10^4 μm^2 for both two electrode types. In details, after patterning the Ti/Au electrodes, the fabricated devices were annealed in N_2 at 200 ℃ for 60 s, in order to achieve better Ohmic contacts [42]. Before the Ni/Au electrodes deposition, the β-Ga_2O_3 thin film was surface treated by O_2 plasmas for 30 s [43-45]. This is because the Schottky contacts on oxide semiconductors are often challenged by the distinct surface charge accumulation layer [42, 44-47]. The metal-semiconductor contact region is the key issue for successful fabrication of Schottky contacts on various oxide semiconductors, including β-Ga_2O_3 studied in this work. The O_2 plasmas treatments allow us to increase the oxygen content at the Ni/β-Ga_2O_3 interface, inducing interface charge reduction for Ni contacts on the surface of β-Ga_2O_3 and the improvement of Schottky characteristics [43, 46, 49, 50]. The current-voltage (I-V) characteristics are performed with a Keithley 4200 semiconductor parameter analyzer. The measurement of time-dependent photoresponse is finished by using an UV lamp with various intensities through tuning the distance between measuring sample and the UV light source, and the UV light intensities could be read by a light receptor and a display instrument. The crystal structure of the β-Ga_2O_3 thin film was analyzed by a Bruker D8 Advance x-ray diffractometer (XRD) with Cu K_α ($\lambda \sim 1.5405$ Å) radiation. All the measurements in this work were executed in air at room temperature.

3. Results and discussion

As shown in figure 1(a), the X-ray diffraction (XRD) pattern of the β-Ga_2O_3 thin film grown by MOCVD on c-plane sapphire substrate indicates a good single crystallinity with highly ordered peaks along $(\bar{2}01)$, $(\bar{4}02)$ and $(\bar{6}03)$ directions (JCPDS #43-1012), except for the sharp (0006) peak from the sapphire substrate (JCPDS #46-1212). Figure 1(b) shows a schematic diagram of the fabricated β-Ga_2O_3 thin film based MSM structured UV solar-blind photodetector. The side length of the quadrate electrode pattern is 400 μm, and the spacing distance between two symmetrical electrodes is 200 μm. So, the efficient UV light radiant area (S) could be calculated to be 8×10^4 μm^2. As key influences on devices output performances, the morphological information of the used β-Ga_2O_3 thin film is provided. The scanning electron microscope (SEM) image is displayed in figure

1(c), the uniformly claviform grains with well-defined boundaries prove good crystallization of the prepared β-Ga_2O_3 thin film. The plane and tridimensional atomic force microscope (AFM) images are shown in figure 2(d) and (e), respectively, the root mean square (RMS) roughness is 1.234 nm.

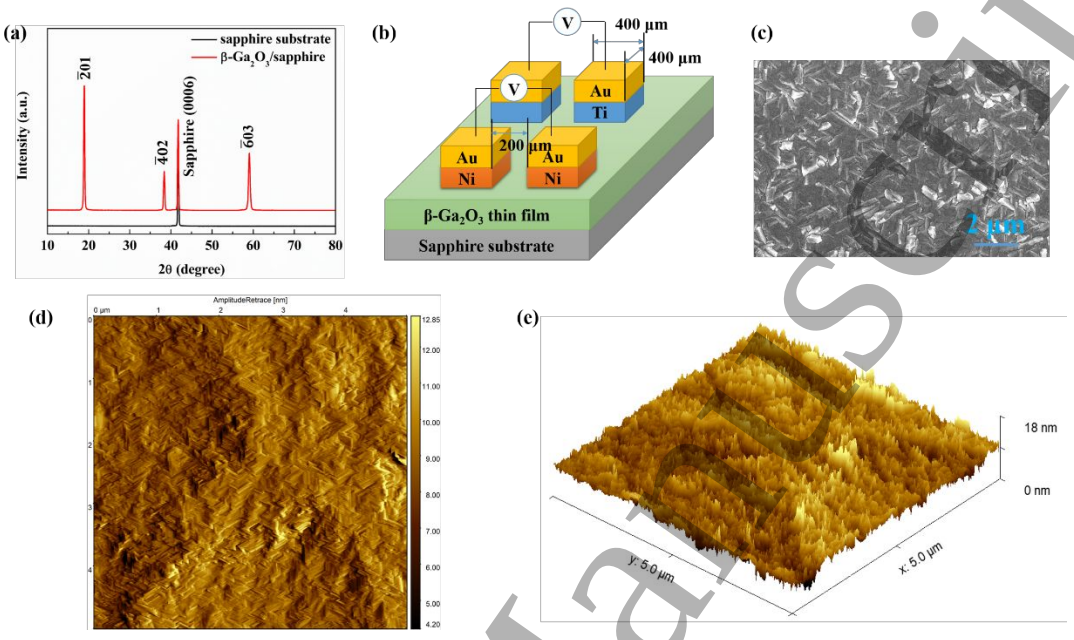

Figure 1. (a) The XRD pattern of the MOCVD-grown β-Ga_2O_3 thin film, (b) the schematic diagram of the fabricated β-Ga_2O_3 thin film based metal-semiconductor-metal (MSM) structured UV solar-blind photodetector. (c) The SEM image of the surface of the β-Ga_2O_3 thin film. (d) Plane AFM surface morphology image of the β-Ga_2O_3 thin films with 5×5 μm^2 scanning area, and the tridimensional AFM image is displayed in (e).

Figure 2(a) shows the dark I-V characteristics of the typical back-to-back MSM structured Schottky and Ohmic β-Ga_2O_3 thin film based UV solar-blind photodetectors, in the voltage range from -5 V to 5 V. The good symmetrical I-V curves suggest a good quality and uniform β-Ga_2O_3 thin film, and consistent electrode patterns. At applied voltage of 5 V, the dark current (I_{dark}) of the Schottky and Ohmic devices are 2.65×10^{-13} A and 9.77×10^{-13} A, respectively. The I_{dark} obtained from Schottky devices is more than four times lower than that from Ohmic devices, due to the efficient constraint of carriers (electrons) transport by the interface barrier of Ni/β-Ga_2O_3, instead of the light sensitive I-V behaviors like a resistor [1, 29]. Seen from figure 2(b), the photocurrent (I_{photo}) at 5 V is 5.58×10^{-8} A and 9.76×10^{-8} A for Schottky and Ohmic devices, respectively, and accordingly the photo-to-dark current ratio $[(I_{photo}-I_{dark})/I_{dark}]$ at 5 V is $\sim 2.1 \times 10^5$ and $\sim 1.0 \times 10^5$. The photoresponse, $(I_{photo}-I_{dark})/I_{dark}$, in Schottky device is superior to that in Ohmic devices, which

is consistent with the description in reference 8. Meanwhile, the I-V curves of both the Ohmic and Schottky contacted photodetectors are shown in figure 2(c) and (d), respectively. Larger UV light intensities contribute to larger I_{photo} for both two typed devices. The "shoulders" in semi-log scale I-V curves of Schottky devices in figure 2(b) maybe due to the non-uniformity Schottky barriers [51]. As indicated in figure 2(c), the I_{photo} of the Ohmic device exhibits a good linear characteristic, suggesting a great stability of UV light response. The incident photons are absorbed in β-Ga_2O_3 thin

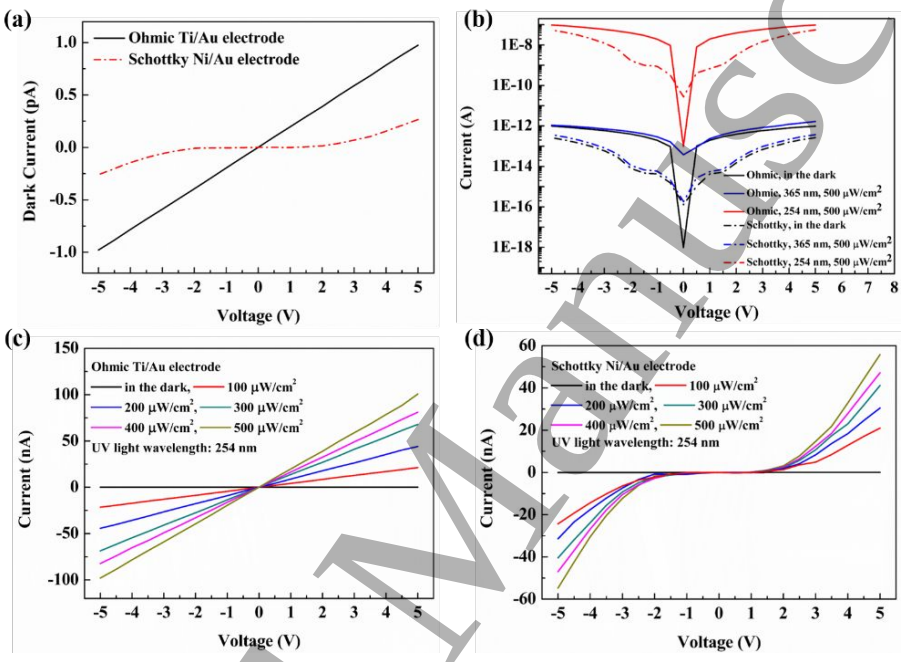

Figure 2. (a) The linear-scale I-V characteristics of the MOCVD-grown β-Ga_2O_3 thin film based photodetector in the dark for Schottky Ni/Au (red dot line) and Ohmic Ti/Au contacts (black full line). (b) The semi log-scale I-V characteristics of both the Schottky (Ni/β-Ga_2O_3/Ni) and Ohmic (Ti/β-Ga_2O_3/Ti) devices in the dark, under the 254 nm and 365 nm UV light illuminations with intensities of 500 μW/cm². The linear-scale I-V curves of (c) Ohmic devices and (d) Schottky devices in the dark and under the 254 nm UV light illuminations with intensities from 100 μW/cm² to 500 μW/cm², step is 100 μW/cm².

film and changed the electronic energy distribution, leading to a disciplinary and linear increase of I_{photo} [1]. The high $(I_{photo}-I_{dark})/I_{dark}$ of ~10^5 and the excellent linearity of I_{photo} verify that the photodetectors presented in this work are sensitive and stable. In addition to the results in figure 2(b), the photocurrent under the 365 nm UV light illumination show a small increase, compared to that in the dark, the small increase maybe due to the defects in β-Ga_2O_3 thin film and/or the unpurified UV light source [14]. This little variation between 365 nm light illumination and dark

condition suggests an outstanding wavelength selectivity, in comparison to the sharp increasing I_{photo} under 254 nm UV light illumination.

Figure 3 shows the time-dependent photoresponse and the voltage-dependent I_{photo} of the β-Ga_2O_3 thin film grown by MOCVD at voltages from 1 V to 5 V under the 254 nm UV light illumination with a light intensity of 500 μW/cm². The I_{photo} increase with the applied voltage increase for both Schottky and Ohmic contacted photodetectors, which can be clearly seen in figure 3(a) and (b). As indicated by figure 3(c), the I_{photo} in Ohmic devices are higher than that in Schottky devices. Taking the time-dependent I_{photo} (5 V and 500 μW/cm²) as an example, the rise and decay time (τ_r and τ_d) of the devices are exhibited and discussed, as displayed in figure 4. In figure 4(a) and (b), the fitting of the time-dependent photo responding curves are according to an exponential relaxation equation [52]:

$$I = I_0 + Ae^{-t/\tau} \quad (1)$$

where I_0 is the stable state photocurrent, A is a constant, t is the time, τ is a relaxation time constant. τ_r and τ_d are the rise and decay edge of the time constants, respectively. In addition, the I_{photo} at different voltages ranging from 1 V to 5 V are shown in figure 4(c). The τ_r and τ_d of Ohmic devices are larger than that of Schottky devices, suggesting a faster photoresponse of Schottky devices compared to that of the Ohmic devices. The faster photoresponse in Schottky devices verifies a rapid change of electron concentration as soon as the UV light is radiated on the surface of the β-Ga_2O_3 thin film, while the slower photoresponse of Ohmic devices maybe due to the electron traps at M-S interface, caused by some defects at the M-S interface and/or in the β-Ga_2O_3 thin film. What could be clearly seen in figure 4(a) and (b) is that the rise edge and decay edge for Schottky and Ohmic devices are different obviously. Using equation (1), the τ_r and τ_d of Ohmic devices are 0.706 s and 0.29 s, respectively, which are larger than those of 0.31 s and 0.156 s of Schottky devices. In detail, the voltage-dependent I_{photo} are given in figure 4(c) and (d), the τ_r and τ_d presented here indicate that the Schottky device has faster photoresponse than the Ohmic devices at the applied voltages range from 1 V to 5 V. Moreover, for these two typed devices, the larger applied voltages could achieve faster photoresponse, i.e., smaller τ_r and τ_d, owing to the larger kinetic energy that electron acquired from higher voltages [12]. In general, the fast light response could be attributed to the rapid change of the electron concentration of the β-Ga_2O_3 thin film as soon as the UV light

was turned on and/or off. For Ohmic (Ti/Au) devices, the response process was deeply affected by the interface trapping and oxygen vacancies defects, therefore, the rise and decay time of the Ohmic devices are long. However, for the Schottky (Ni/Au) devices after O_2 plasmas treatments at the Ni/β-Ga_2O_3 interface, decent Schottky electrical behaviors were obtained, and also, the electrons can be photogenerated and recombined faster than that of the Ohmic devices, due to the weaker influences of traps and defects on the light responses [8, 53-55].

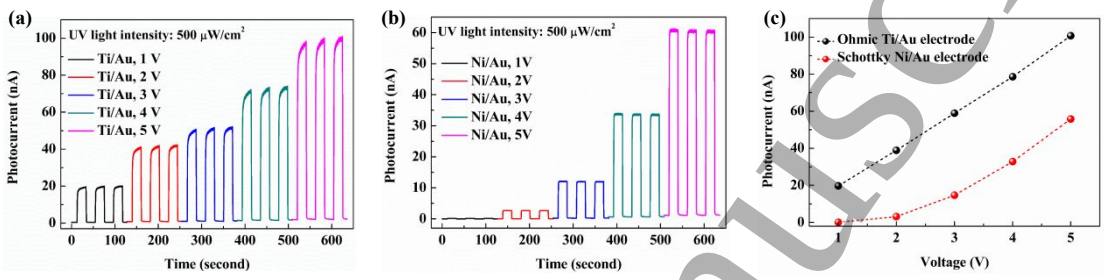

Figure 3. The continuous time-dependent photoresponse of the β-Ga_2O_3 thin film grown by MOCVD at voltages from 1 V to 5 V under the 254 nm UV light illumination with a light intensity of 500 μW/cm² for (a) Ohmic devices and (b) Schottky devices. (c) The voltage-dependent photocurrents under the 254 nm UV light illumination with a light intensity of 500 μW/cm².

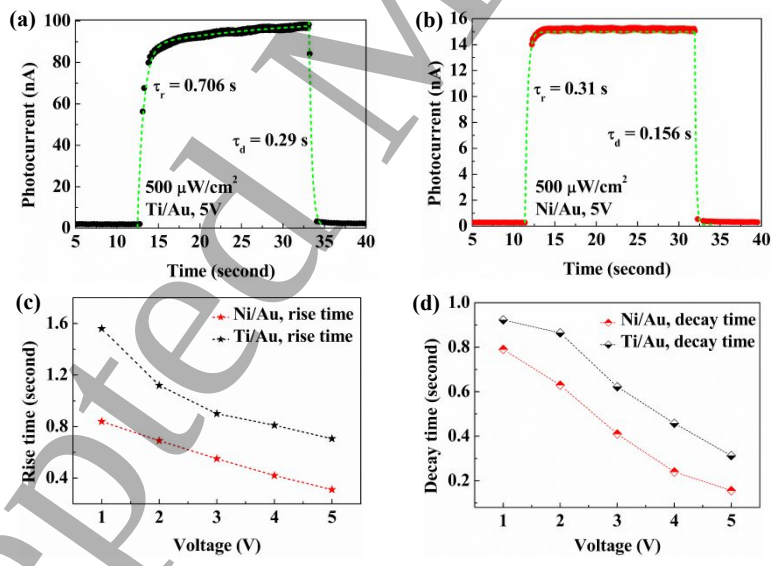

Figure 4. The rise and decay time of the β-Ga_2O_3 thin film based photodetector of (a) Ohmic devices and (b) Schottky devices responding to the 254 nm UV light with a light intensity of 500 μW/cm² at 5 V, with Ti/Au and Ni/Au electrodes, respectively. The voltage-dependent (c) rise time and (d) decay time for Schottky and Ohmic devices.

As reported, the band structure of β-Ga_2O_3 along a continuous path in the Brillouin zone has been studied [56-59]. According to these results, the conduction-band minimum β-Ga_2O_3 material

is located at Γ point, and the corresponding bandgap is only about 0.04 eV larger than those at other points in the band structure [57]. In addition, the secondary conduction bands at Z and Y points just have minimal values, as well as the minima at N and X points. So the bandgap of β-Ga_2O_3 is direct with an acceptable deviation [56-59] at every points in its energy band structure. For understanding the inherent physical mechanism of the operating Schottky Ni/Au contacted and Ohmic Ti/Au contacted β-Ga_2O_3 photodetectors, the systematic band diagrams of β-Ga_2O_3 with Ti and Ni in the dark and under the 254 nm UV light illumination are shown in figure 5(a)-(d). The work functions of Ti and Ni [Φ(Ti) and Φ(Ni)] are 4.33 eV and 5.15 eV, respectively, and the electron affinity of β-Ga_2O_3 [χ(β-Ga_2O_3)] is about 4.00 eV as reported [60-62]. So, the interface barriers of β-Ga_2O_3 with Ti and Ni ($\Delta\varphi_{Ti-\beta-Ga2O3}$ and $\Delta\varphi_{Ni-\beta-Ga2O3}$) could be calculated to be 0.33 eV and 1.15 eV, on the basis of the Schottky-Mott rule [29, 30]. The puny interface barrier between Ti and β-Ga_2O_3 contributes to the Ohmic M-S contact, while the larger interface barrier between Ni and β-Ga_2O_3 leads to the Schottky M-S contact. The I-V behavior of Ohmic devices could be expressed by the electron tunneling, while for the Schottky contact, the I-V characteristic could be described by the thermionic emission (TE) theory [63-65]:

$$J = J_0\left(\exp\left(\frac{qV}{nkT}\right) - 1\right) \quad (2)$$

and

$$J_0 = A^* T^2 \exp\left(-\varphi_B/kT\right) \quad (3)$$

where J_0 is the saturation current density, A is the area of M-S contact, A^* is the efficient Richardson constant ($A^* = \frac{4\pi q m^* k^2}{h^3} = 41.1\ A/cm^2 \cdot K^2$) by taking m^* of $0.342m_0$, m_0 is the free electron mass of β-Ga_2O_3 [66, 67], k is Boltzmann constant, and φ_B is the barrier height and expressed as $\varphi_B = \frac{kT}{q}\ln\left(\frac{A^* T^2}{J_0}\right)$. As displayed in figure 5, the built-in electrical field ($V_{built\text{-}in}$) is developed when the Ni and β-Ga_2O_3 contacts. In the dark, as shown in figure 5(a) and (c), the larger interface barrier in Schottky device could restrict electron transport across the Ni/β-Ga_2O_3 interface, while the Ohmic device is almost like a radiation (UV light)-sensitive resistor with tiny interface barrier. Therefore, the I_{dark} in Ohmic device is larger than that in Schottky device as displayed in figure 2(a), and the Schottky device may be more sensitive to the small signal owing to its smaller I_{dark}. Under 254 nm UV light illuminations, as displayed in figure 5(b) and (d), the incident photons

with energy (hν) greater than the energy bandgap of the β-Ga_2O_3 thin film could be absorbed by the β-Ga_2O_3 material and then produce the photo-generated electron-hole pairs (electrons at valence band are motivated to the conduction band by absorbed photons, and correspondingly holes are produced at the valence band), thereby changing the electrical conductivity of β-Ga_2O_3. Given a voltage, the electrons in β-Ga_2O_3 are pushed to the conduction band, while the holes are driven to the valence band. For Ohmic Ti/Au contacted β-Ga_2O_3 photodetector studied here, the I_{photo} is linearly improved by the incident 254 nm UV light. While for the Schottky Ni/Au contacted β-Ga_2O_3 photodetector, the I-V characteristics show Schottky (rectifying) behaviors owing to the interface barrier between Ni metal electrode and β-Ga_2O_3 thin film. This phenomenon could be obtained whether the 254 nm UV light is turned on or not [1].

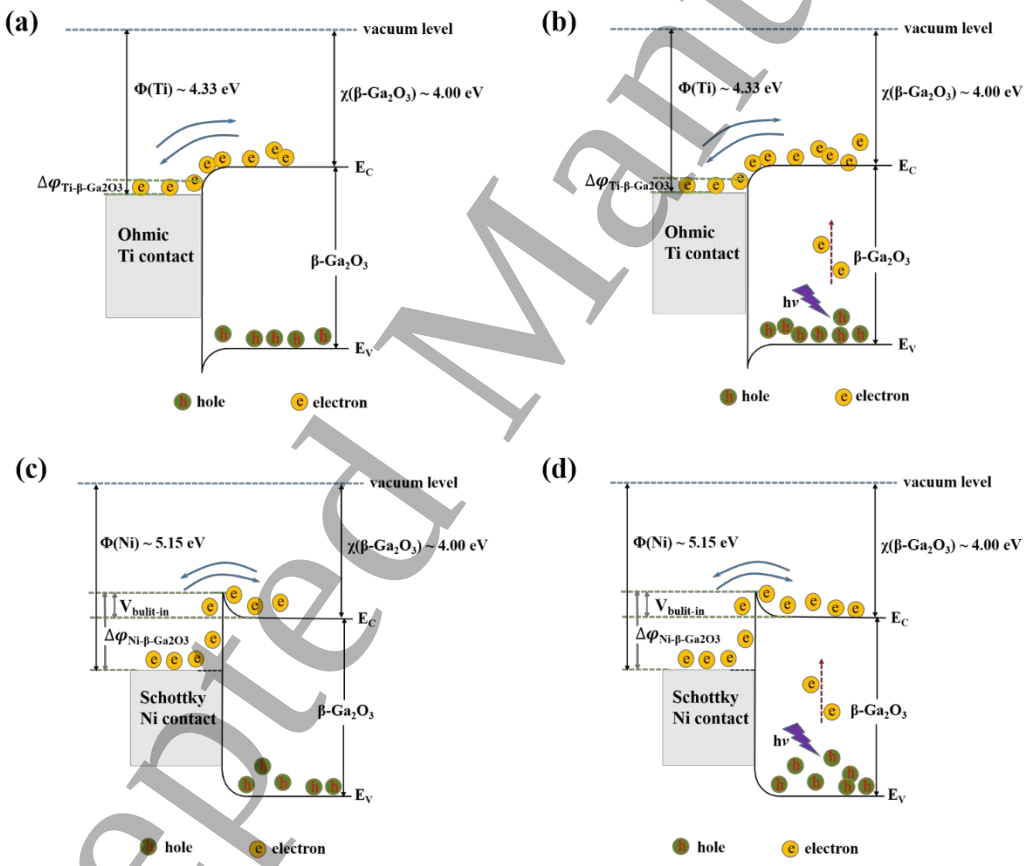

Figure 5. Band diagram of the β-Ga_2O_3 with Ti (a) in the dark and (b) under the 254 nm light illumination. Band diagram of the β-Ga_2O_3 with Ni (c) in the dark and (d) under the 254 nm light illumination.

For photodetectors, responsivity (R) and detectivity (D^*) are two vital parameters to evaluate the detector performances and could be described as following relationships [68]:

$$R = \frac{I_{photo} - I_{dark}}{P_{light} \cdot S} \quad (4)$$

and

$$D^* = \frac{R_{254}}{\sqrt{2qI_{dark}/S}} \quad (5)$$

where P_{light} is the UV light intensity used in the measurements, S is the efficient radiant area in devices, R_{254} is the photo responsivity under 254 nm light illumination. According to equation (4) and (5), the R and D^* by different driven voltages and light intensities are displayed in figure 6(a)-(d) for Schottky and Ohmic β-Ga_2O_3 thin film based UV solar-blind photodetectors. Seen from figure 6(a), with the UV light intensity of 500 μW/cm^2, the responsivities increase with the increasing voltages from 1 V to 5 V, for both the Schottky (from 1.68 mA/W to 0.14 A/W) and Ohmic (from 49 mA/W to 0.25 A/W) devices. The responsivities for Ohmic devices ranging from 1 V to 5 V are all higher than those of Schottky devices, due to the larger I_{photo} of Ohmic devices compared to the Schottky devices, as well as the same P_{light} intensities and S, following the description in equation (4). In addition to the responsivities with different UV light intensities, the R of Ohmic devices are also higher than those of Schottky devices, as shown in figure 6(c). The responsivities are increased by the increasing light intensity. By contrast, the Ohmic device could make more photogenerated electron-hole pairs to generate I_{photo} than the Schottky devices [1, 69-72].

While the detectivies are governed by responsivities and the square root of I_{dark} for a photodetector, as given in equation (5). As shown in figure 6(b), the D^* of Schottky devices are larger than that of Ohmic devices, owing to superlow I_{dark} (3.2×10^{-16} A) of Schottky devices at 1 V, which should be contributed to the rectifying effect caused by the Ni/β-Ga_2O_3 interface barrier. In comparison, the D^* of Schottky device at 2 V to 5 V are obviously smaller than that at 1 V, this trend is in accordance with the rectifying I-V curves in figure 2(d). For Ohmic devices, the I_{dark} is always kept at ~ 10^{-13}, so the D^* have the same evolutive tendency with R as displayed in figure 6(a). In figure 6(d), the D^* of Schottky devices are slightly larger than those of Ohmic devices at 5 V with 254 nm UV light intensity from 100 μW/cm^2 to 500 μW/cm^2 with a step of 100 μW/cm^2, in accordance with the results in figure 6(b) at 5 V, indicating a better characterizing parameter for normalizing signal-to-noise ratio [1].

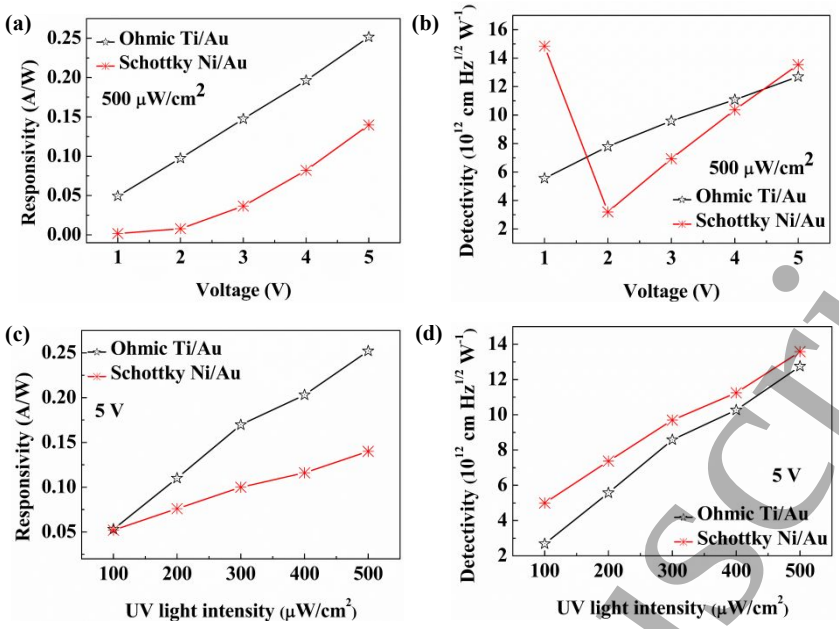

Figure 6. The voltage-dependent (a) responsivity and (b) detectivity for both Schottky Ni/Au and Ohmic Ti/Au contacted β-Ga_2O_3 thin film based UV solar-blind photodetectors with 254 nm UV light intensity of 500 μW/cm^2 from 1 V to 5 V with a step of 1 V. The UV light intensity-dependent (c) responsivity and (d) detectivity for both Schottky Ni/Au and Ohmic Ti/Au contacted β-Ga_2O_3 thin film based UV solar-blind photodetectors at 5 V with 254 nm UV light intensities from 100 μW/cm^2 to 500 μW/cm^2 with a step of 100 μW/cm^2.

4. Conclusions

In summary, in this study, we grew β-Ga_2O_3 thin film by using metal-organic chemical vapor deposition technique, and made a comparison of optoelectrical properties of the prepared β-Ga_2O_3 thin films with Schottky Ni/Au and Ohmic Ti/Au contacted electrodes. The results show that Schottky device has higher photo-to-dark current ratios, and faster photo response speed than those of the Ohmic device. Working as a UV solar-blind photodetector, the responsivities of Schottky devices are larger than those of Ohmic devices. Owing the lower I_{dark}, the D^* of Schottky devices are superior to those of Ohmic devices at 5 V with light intensity from 100 to 500 μW/cm^2. What's more, with 500 μW/cm^2 light intensity, the different D^* from 1 V to 5 V are also discussed on the basis of the Schottky I-V behaviors. In a word, we discussed and analyzed the differences between Schottky and Ohmic contacted β-Ga_2O_3 thin film based UV solar-blind photodetectors, and give out some inherent physical mechanism, in order to present the effect of metal-β-Ga_2O_3 contacted types (Schottky or Ohmic) on the devices performances, as well as their differences, operating as a UV solar-blind photodetector.

Acknowledgments

This work was supported by the National Natural Science Foundation of China (Grant Nos. 61774019, 51572033, and 51572241), the Beijing Municipal Commission of Science and Technology, China (Grant No. SX2018-04). In addition, the authors acknowledged the Fundamental Research Funds for the Central Universities and the Foundation of State Key Laboratory of Information Photonics and Optical Communications (Beijing University of Posts and Telecommunications).

References

1. Razeghi M and Rogalski A 1996 *J. Appl. Phys.* **79** 7433
2. Chen H, Liu K, Hu L, Al-Ghamdi A A and Fang X 2015 *Mater. Today* **18** 493
3. Sang L, Liao M and Sumiya M 2013 *Sensors* **13** 10482
4. Konstantatos G and Sargent E H 2010 *Nat. Nanotechnol.* **5** 391
5. Pearton S J, Yang J, Cary P H, Ren F, Kim J, Tadjer M J and Mastro M A 2018 *Appl. Phys. Rev.* **5** 011301
6. Liu Z, Li P G, Zhi Y S, Wang X L, Chu X L and Tang W H 2019 *Chin. Phys.* B **28** 017105
7. Xu J, Zheng W and Huang F 2019 *J. Mater. Chem.* C **7** 8753
8. Guo D Y, Wu Z P, An Y H, Guo X C, Chu X L, Sun C L, Li L H, Li P G and Tang W H 2014 *Appl. Phys. Lett.* **105** 023507
9. Kumar N, Arora K and Kumar M 2019 *J. Phys. D: Appl. Phys.* **52** 335103
10. Qin Y, Sun H, Long S, Tompa G S, Salagaj T, Dong H, He Q, Jian G, Liu Q, Lv H and Liu M 2019 *IEEE Electron Device Lett.* **40** 1475
11. Xu Y, Chen X, Zhou D, Ren F, Zhou J, Bai S, Lu H, Gu S, Zhang R, Zheng Y and Ye J 2019 *IEEE Trans. Electron Devices* **66** 2276
12. Liu Z, Wang X, Liu Y, Guo D, Li S, Yan Z, Tan C -K, Li W, Li P and Tang W 2019 *J. Mater. Chem. C* **7** 13920
13. Chen X, Mu W, Xu Y, Fu B, Jia Z, Ren F, Gu S, Zhang R, Zheng Y, Tao X and Ye J 2019 *ACS Appl. Mater. Interfaces* **11** 7131
14. Dong L, Yu J, Jia R, Hu J, Zhang Y and Sun J 2019 *Opt. Mater. Express* **9** 1191
15. Oshima T, Okuno T, Arai N, Suzuki N, Ohira S and Fujita S 2008 *Appl. Phys. Express* **1** 011202
16. Chen M, Ma J, Li P, Xu H and Liu Y 2019 *Opt. Express* **27** 8717
17. Zou R, Zhang Z, Liu Q, Hu J, Sang L, Liao M and Zhang W 2014 *Small* **10** 1848
18. Wang S, Chen K, Zhao H, He C, Wu C, Guo D, Zhao N, Ungar G, Shen J, Chu X, Li P and Tang W H 2019 *RSC Adv.* **9** 6064
19. Feng W, Wang X, Zhang J, Wang L, Zheng W, Hu P, Cao W and Yang B 2014 *J. Mater. Chem. C* **2** 3254
20. Li Y, Tokizono T, Liao M, Zhong M, Koide Y, Yamada I and Delaunay J 2010 *Adv. Funct. Mater.* **20** 3972

21. An Y H, Guo D Y, Li S Y, Wu Z P, Huang Y Q, Li P G, Li L H and Tang W H 2016 *J. Phys. D: Appl. Phys.* **49** 285111
22. Liu Z, Wang X, Zhi Y S, Wang X L, Chu X L, Li S, Yan Z, Li P G and Tang W H 2019 *Phys. Status Solidi* A 1900570, [doi: 10.1002/pssa.201900570]
23. Guo D Y, Shi H Z, Qian Y P, Lv M, Li P G, Su Y L, Liu Q, Chen K, Wang S L, Cui C, Li C R and Tang W H 2017 *Semicond. Sci. Technol.* **32** 03LT01
24. Guo D, Su Y, Shi H, Li P, Zhao N, Ye J, Wang S, Liu A, Chen Z, Li C and Tang W 2018 *ACS Nano* **12** 12827
25. Kong W Y, Wu G A, Wang K Y, Zhang T F, Zou Y F, Wang D D and Luo L B 2016 *Adv. Mater.* **28** 10725
26. Li S, Guo D, Li P, Wang X, Wang Y, Yan Z, Liu Z, Zhi Y, Huang Y, Wu Z and Tang W 2019 *ACS Appl. Mater. Interfaces* **11** 35105
27. Sze S M, Coleman D J and Loya A 1971 *Solid-State Electron.* **14** 1209
28. Xue H W, He Q M, Jian G Z, Long S B, Pang T and Liu M 2018 *Nanoscale Res. Lett.* **13** 290
29. Mott N F 1939 *Proc. R. Soc. (London)* A **171** 27
30. Schottky W 1939 *Z. Phys.* **113** 367
31. Sze S M and Ng K K 2007 *Physics of Semiconductor Devices* (NJ: John Wiley & Sons, Inc.)
32. Bae J, Kim H Y and Kim J 2017 *ECS J. Solid State Sci. Technol.* **6** Q3045
33. An Y H, Guo D Y, Li Z M, Wu Z P, Zhi Y S, Cui W, Zhao X L, Li P G and Tang W H 2016 *RSC Adv.* **6** 66924
34. Chen X, Liu K, Zhang Z, Wang C, Li B, Zhao H, Zhao D and Shen D 2016 *ACS Appl. Mater. Interfaces* **8** 4185
35. Cowley A M and Sze S M 1965 *J. Appl. Phys.* **36** 3212
36. Mönch W 1970 *Surf. Sci.* **21** 443
37. Tung R T 1992 *Phys. Rev.* B **45** 13509
38. Jiao Y, Hellman A, Fang Y, Guo S and Kall M 2015 *Sci. Rep.* **5** 11374
39. Li J G 1997 *Mater. Chem. Phys.* **47** 126
40. Thomson G W 1946 *Chem. Rev.* **38** 1
41. Li Z, Jiao T, Hu D, Lv Y, Li W, Dong X, Zhang Y, Feng Z and Zhang B 2019 *Coatings* **9** 281
42. Mao S and Luo J 2019 *J. Phys. D: Appl. Phys.* **52** 503001
43. Michel J, Splith D, Rombach J, Papadogianni A, Berthold T, Krischok S, Grundmann M, Bierwagen O, von Wenckstern H and Himmerlich M 2019 *ACS Appl. Mater. Interfaces* **11** 27073
44. Yang J, Sparks Z, Ren F, Pearton S J and Tadjer M 2018 *J. Vac. Sci. Technol.* B **36** 061201
45. Schultz T, Vogt S, Schlupp P, von Wenckstern H, Koch N and Grundmann M 2018 *Phys. Rev. Applied* **9** 064001
46. King P D C, Veal T D, Payne D J, Bourlange A, Egdell R G and McConville C F 2008 *Phys. Rev. Lett.* **101** 116808
47. Hämäläinen J, Munnik F, Ritala M and Leskelä M 2008 *Chem. Mater.* **20** 6840
48. Fleisch T H and Mains G J 1986 *J. Phys. Chem.* A **90** 5317
49. Splith D, Müller S, von Wenckstern H and Grundmann M 2018 *Proc. SPIE* **10533** 10533C
50. Hou C, Gazoni R M, Reeves R J and Allen M W 2019 *IEEE Electron Device Lett.* **40** 337
51. Jian G, He Q, Mu W, Fu B, Dong H, Qin Y, Zhang Y, Xue H, Long S, Jia Z, Lv H, Liu Q, Tao X and Liu M 2018 *AIP Adv.* **8** 015316

52. Liu N, Fang G, Zeng W, Zhou H, Cheng F, Zheng Q, Yuan L, Zou X and Zhao X 2010 *ACS Appl. Mater. Interfaces* **2** 1973
53. Mosbacker H L, Strzhemechny Y M, White B D, Smith P E, Look D C, Reynolds D C, Litton C W and Brillson L J 2005 *Appl. Phys. Lett.* **87** 012102
54. Allen M W and Durbin S M 2008 *Appl. Phys. Lett.* **92** 122110
55. Moloney J, Tesh O, Singh M, Roberts J W, Jarman J C, Lee L C, Huq T N, Brister J, Karboyan S, Kuball M, Chalker P R, Oliver R A and Massabua F C –P 2019 *J. Phys. D: Appl. Phys.* **52** 475101
56. Wang X L, Quhe R G, Zhi Y S, Liu Z, Huang Y Q, Dai X Q, Tang Y N, Wu Z P and Tang W H 2019 *Superlattices Microstruct.* **125** 330
57. Peelaers H and Van de Walle C G 2015 *Phys. Status Solidi* B **252** 828
58. Varley J B, Weber J R, Janotti A and Van de Walle C G 2010 *Appl. Phys. Lett.* **97** 142106
59. He H, Blanco M A and Pandey R 2006 *Appl. Phys. Lett.* **88** 261904
60. Michaelson H B 1977 *J. Appl. Phys.* **48** 4729
61. Mohamed M, Irmscher K, Janowitz C, Galazka Z, Manzke R and Fornari R 2012 *Appl. Phys. Lett.* **101** 132106
62. Darowicki K, Krakowiak S and Slepski P 2006 *Electrochim. Acta* **51** 2204
63. Furno M, Bonani F and Ghione G 2007 *Solid-State Electron.* **51** 466
64. Latreche A 2019 *SN Appl. Sci.* **1** 188
65. Harada T, Ito S and Tsukazaki 2019 *Sci. Adv.* **5** eaax5733
66. He H, Orlando R, Blanco M A, Pandey R, Amzallag E, Baraille I and Rerat M 2006 *Phys. Rev.* B **74** 195123
67. Sasaki K, Higashiwaki M, Kuramata A, Masui T and Yamakoshi S 2013 *IEEE Electron Device Lett.* **34** 493
68. Gong X, Tong M, Xia Y, Cai W, Moon J S, Cao Y, Yu G, Shieh C L, Nilsson B and Heeger A J 2009 *Science* **325** 1665
69. Rose A 1963 *Concepts in Photoconductivity and Allied Problems* (NY: Inter-science)
70. Rettie A J E, Chemelewski W D, Emin D and Mullins C B 2016 *J. Phys. Chem. Lett.* **7** 471
71. Kokum A F, Miranowicz A, Liberato S D, Savasta S and Nori F 2019 *Nat. Rev. Phys.* **1** 19
72. Latreche A and Ouennoughi Z 2013 *Semicond. Sci. Technol.* **28** 105003